Electronic Supplementary Material (ESI) for Analyst.

Supporting Information

Investigation of the interactions between methylene blue and intramolecular G-quadruplexes: an explicit distinction in electrochemical behavior

Ting Cao,[a] Fang-Ting Zhang,[a] Liang-Yuan Cai,[a] Ying-Lin Zhou,[a] Niklaas J. Buurma,*[b] and Xin-Xiang Zhang*[a]*

[a]. Beijing National Laboratory for Molecular Sciences (BNLMS), MOE Key Laboratory of Bioorganic Chemistry and Molecular Engineering, College of Chemistry, Peking University
No.202 Chengfu Road, Haidian District, Beijing 100871, China
E-mail: zhouyl@pku.edu.cn, zxx@pku.edu.cn

[b]. Physical Organic Chemistry Centre, School of Chemistry, Cardiff University, Main Building, Park Place, Cardiff, CF10 3AT (UK)
E-mail: buurma@cardiff.ac.uk

Table S1 Intramolecular G-Quadruplex sequence information

name	sequence (5' to 3')	extinction coefficient[b] / L·mole^{-1}·cm^{-1}	description
TA	GGTTGGTGTGGTTGG	143300	thrombin aptamer[1]
TA2	GGGGTTGGGGTGTGGGGTTGGGG	224100	4-plane aptamer[2]
HT	AGGGTTAGGGTTAGGGTTAGGG	228500	human telomere[3]
Oxy28	GGGGTTTTGGGGTTTTGGGGTTTTGGGG	262000	Oxytrichia telomeric[3]
Bcl-2	GGGCGCGGGAGGAAGGGGGCGGG	231300	B-cell CLL/lymphoma[4]
PS2.M	GTGGGTAGGGCGGGTTGG	177400	hemin aptamer[5]
EAD4	CTGGGTTGGGTTGGGTTGGGA	200700	designed sequence[6]
VEGF	GGGCGGGCCGGGGGCGGG	169800	vascular endothelial growth factor[7]
RET	GGGCGGGCGCGGGCGGG	159100	RET oncogene[8]
c-Myc	TGAGGGTGGGGAGGGTGGGGAA	229900	human c-myc gene[9]
c-Kit21	CGGGCGGGCGCGAGGGAGGGG	205600	c-kit gene promoter[10]
EAD2	CTGGGAGGGAGGGAGGGA	189900	designed sequence[6]

RDNA[a]	GCTATGACTCACCGTGCC	162100	random sequence

[a]RDNA denotes a random DNA sequence which does not form a G-quadruplex structure. [b]Extinction coefficients are obtained from a free website: http://sg.idtdna.com/calc/analyzer.

Table S2. The conformations of different intramolecular G-quadruplexes and their CD spectra in the absence and presence of MB at room temperature.

Conformation type	name	CD spectra of G-quadruplexes in the absence and presence of MB
Antiparallel type	TA	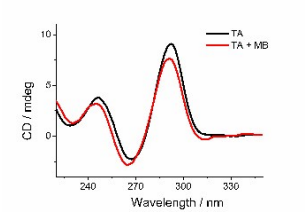
	TA2	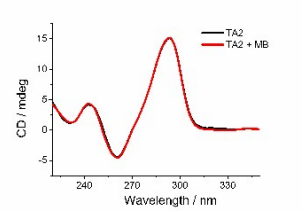
	Oxy28	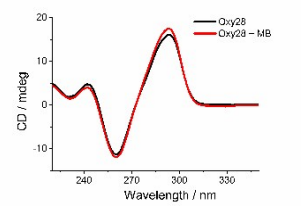
Mixed type	HT	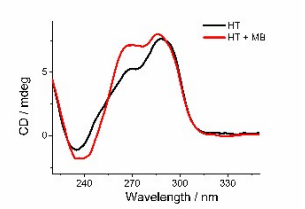
	Bcl-2	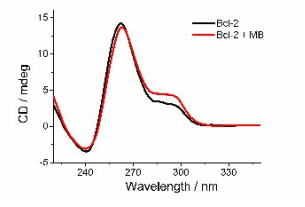

Parallel type	PS2.M	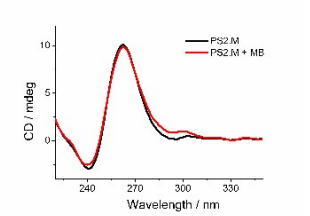
	VEGF	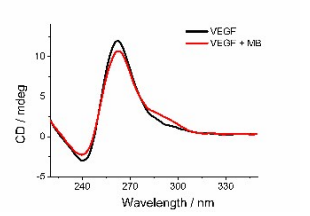
	RET	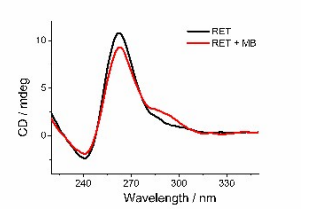
	c-myc	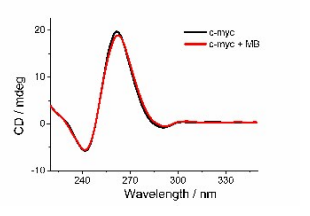
	c-Kit21	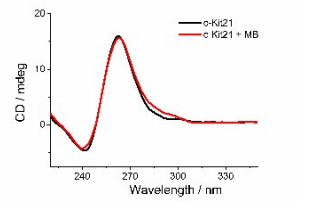
	EAD4	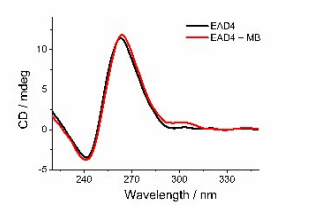

	EAD2	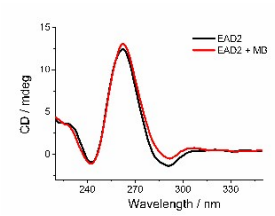
NO G-quadruplex	RDNA	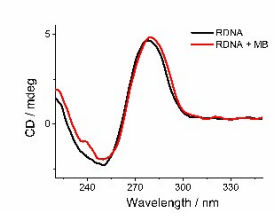

For all the CD measurements, the concentrations of G-quadruplexes and MB were 20 μM and 200 μM, respectively.

Table S3 SWV behavior of MB in the presence of different G-quadruplexes

G-quadruplex species	E_p / V	i_p / nA[a]	Structure type
MB	-0.272	198.5 (2.2)	
MB+RDNA	-0.268	161.8 (0.4)	single strand
MB+TA	-0.272	151.6 (0.5)	antiparallel
MB+TA2	-0.268	122.7 (0.4)	antiparallel
MB+Oxy28	-0.272	111.8 (2.0)	antiparallel
MB+HT	-0.272	116.1 (0.7)	coexisting or mixed hybrid type
MB+Bcl-2	-0.272	93.3 (0.3)	coexisting or mixed hybrid type
MB+VEGF	-0.272	111.5 (1.3)	parallel
MB+RET	-0.272	105.1 (0.8)	parallel
MB+PS2.M	-0.272	99.2 (1.1)	parallel
MB+c-Kit21	-0.268	91.9 (1.5)	parallel
MB+EAD2	-0.268	87.9 (0.2)	parallel
MB+c-Myc	-0.272	80.2 (0.2)	parallel
MB+EAD4	-0.272	70.7 (0.8)	parallel

[a]Numbers in parentheses are standard deviations for three measurements.

Table S4. Cyclic voltammetric data of MB in the absence and presence of DNA

	R	E_{pa}/V	E_{pc}/V	ΔE_p/ mV	$E_{1/2}$/V	i_{pa}/nA	i_{pc}/nA	i_{pa}/ i_{pc}
	0	-0.205	-0.280	75	-0.242	55.6	97.41	0.57
	0.5	-0.240	-0.315	75	-0.278	6.637	31.72	0.21
	1		-0.315				23.32	
EAD2	2		-0.320				16.56	
	5		-0.310				10.18	
	8		-0.310				7.38	
	10		-0.315				5.58	
	0	-0.210	-0.280	70	-0.245	54.59	91.93	0.59
	0.5	-0.225	-0.300	75	-0.262	32.28	60.69	0.53
	1	-0.220	-0.305	85	-0.262	29.45	56.33	0.52
RDNA	2	-0.225	-0.305	80	-0.265	23.49	50.06	0.48
	5	-0.220	-0.300	80	-0.260	21.55	44.46	0.53
	8	-0.225	-0.300	75	-0.262	21.73	40.43	0.54
	10	-0.225	-0.300	75	-0.262	20.11	37.92	0.53

Figure S1 Schematic of miniaturized electrochemical device with a three-electrode system. Ag/AgCl was used as reference electrode, Pt wire was used as counter electrode and a carbon fiber packaged in a glass tube was used as working electrode.

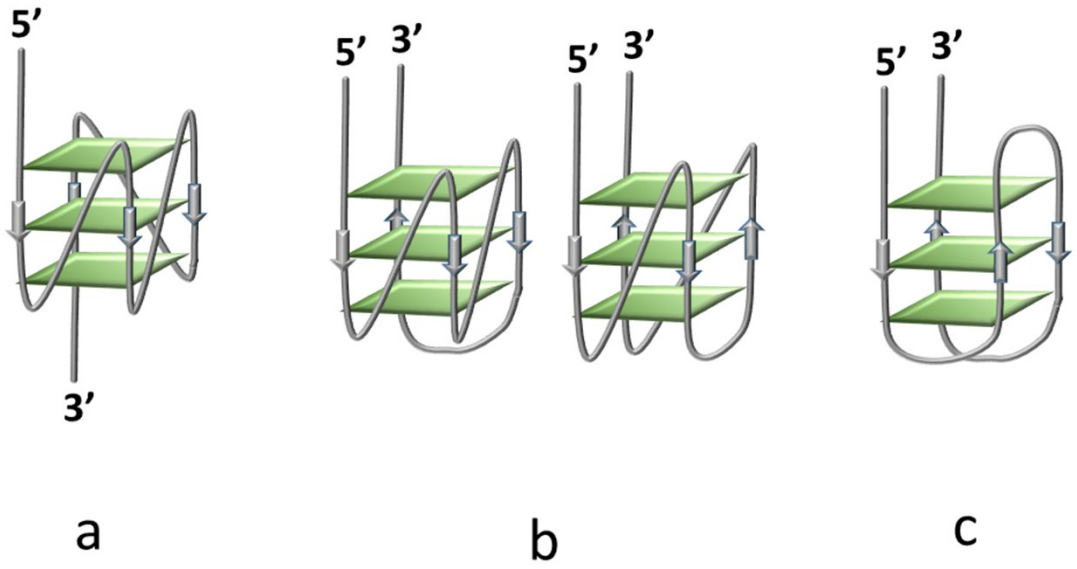

Figure S2 Representative schematic of different conformations of G-quadruplex (a) parallel type, (b) mixed hybrid type and (c) antiparallel type.

From the orientation of the nucleic acids from 5’ to 3’, for parallel G-quadruplex, all strands of quadruplex stem are in the same direction. For antiparallel G-quadruplex, all adjacent strands of quadruplex stem are in the opposite direction. And for mixed hybrid G-quadruplex, the strands of quadruplex stem possess at least one strand with opposite direction.

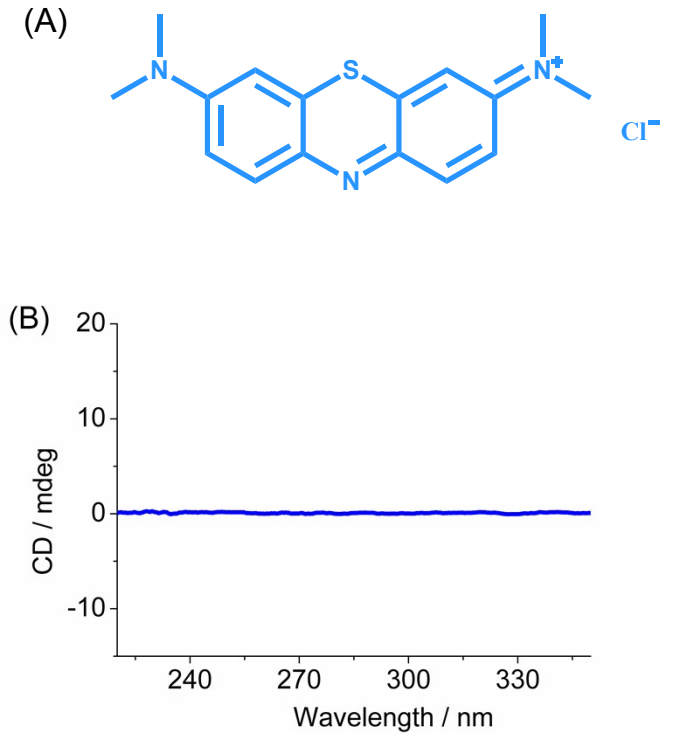

Figure S3 (A) The structure of MB, (B) CD absorption spectrum of MB at 220-350 nm.

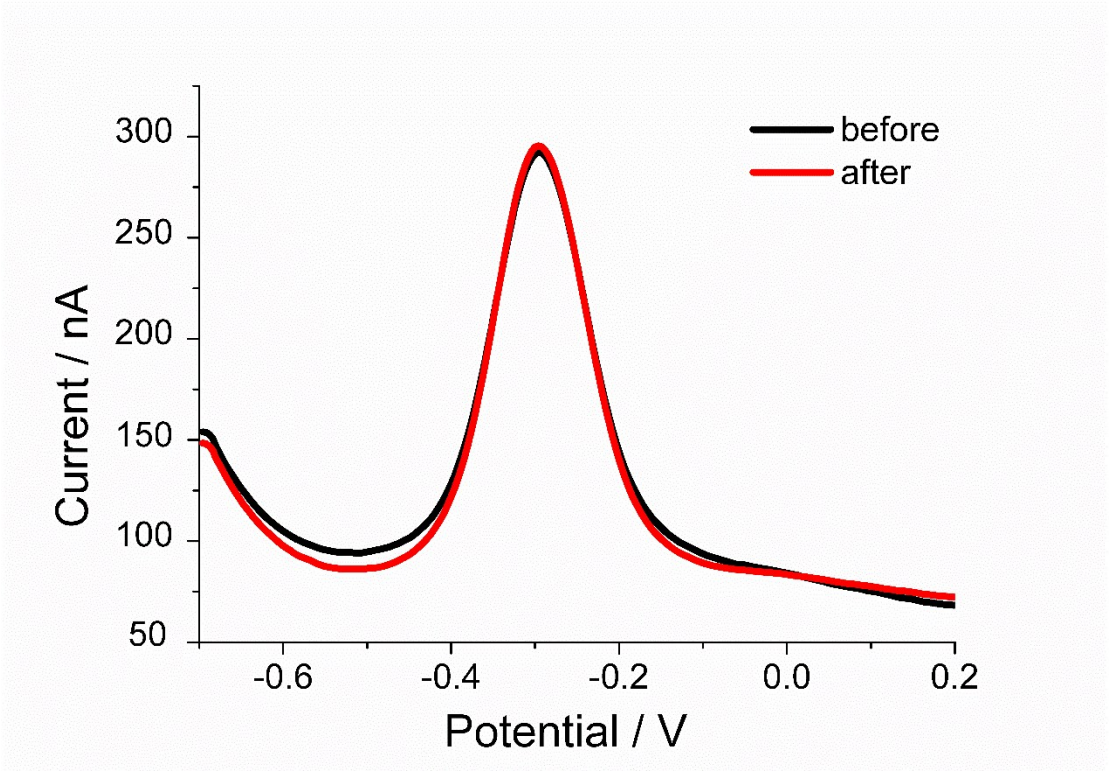

Figure S4 SWV of 10 μM MB before and after measurements of samples containing different intramolecular G-quadruplexes and MB.

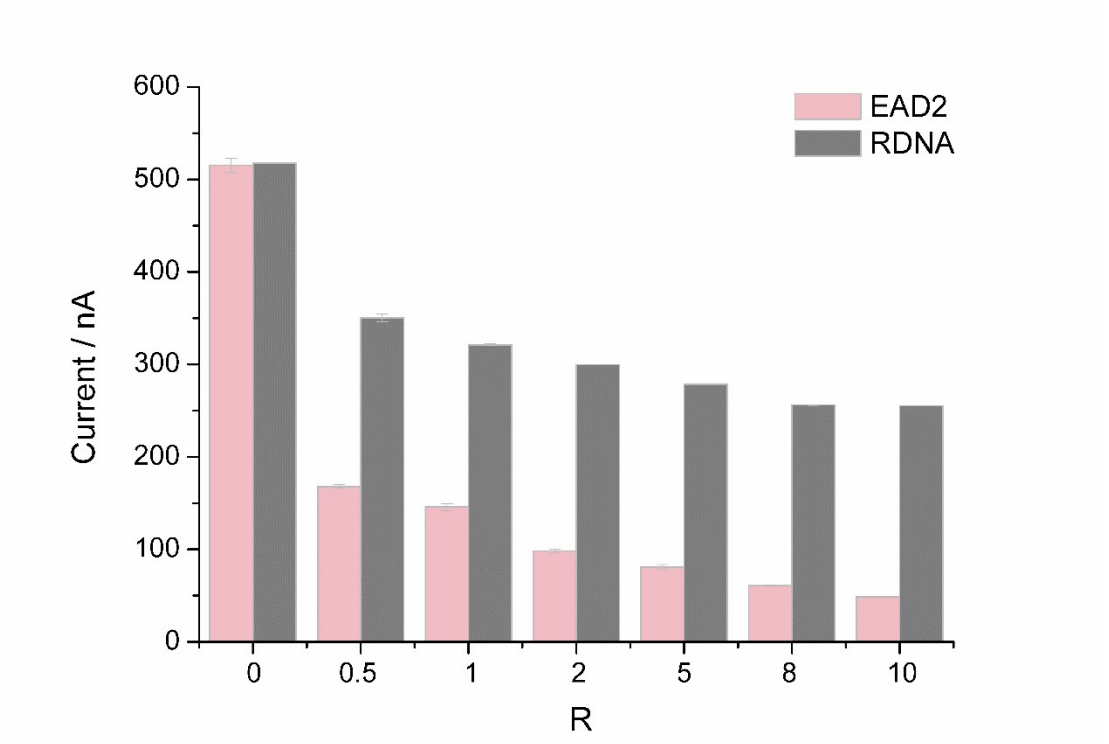

Figure S5 The diffusing current of MB in the presence of DNA with different R by SWV (PB buffer, sweep rate of 800 mV/s, R is the concentration ratio of DNA to MB)

ITC data analysis

The interaction model used for the data analysis involves isosdesmic self-aggregation of MB (with thermodynamic parameters Kagg and DHagg) in combination with either one (thermodynamic parameters K_{A1}, ΔH_{A1}, n_{A1}) or two binding sites (thermodynamic parameters K_{A1}, ΔH_{A1}, n_{A1} and K_{B1}, ΔH_{B1}, n_{B1}) available on the quadruplex structures (Scheme 1).

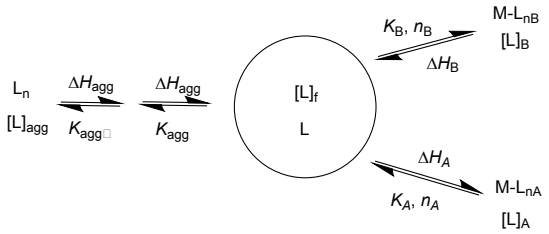

Scheme 1 Ligand aggregation and two different DNA-ligand binding events

During data analysis, parameter values were restricted to the following ranges, unless indicated otherwise. Enthalpies were restricted to the range [-5×10^5 – $+5\times10^5$] cal mol^{-1}; equilibrium constants are restricted to the range [1 – 6×10^{20}] M^{-1} with the second equilibrium constant restricted to values smaller than the first equilibrium constant to avoid swap-overs; the stoichiometries were restricted to the range [0.0002 – 20] molecules per nucleic acid unit.

ITC study of MB self aggregation

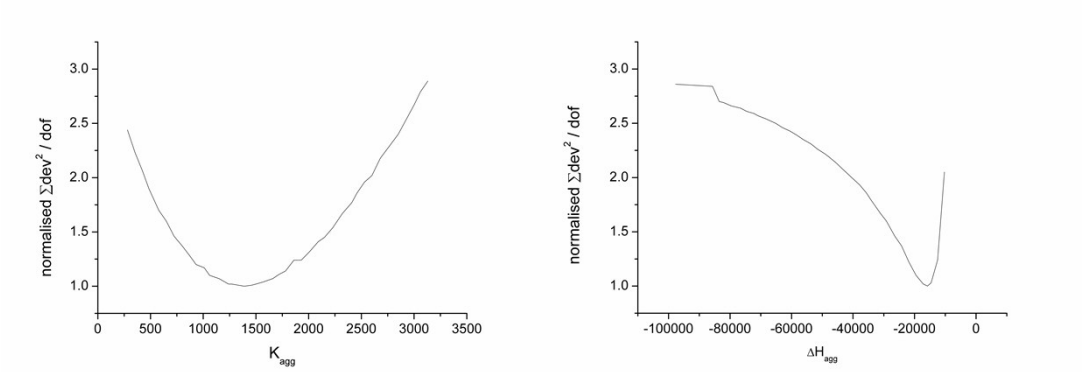

Figure S6 Evaluation of error margins for K_{agg} and ΔH_{agg} for the calorimetric dilution experiment.

Values of K_{agg} and ΔH_{agg} for which the normalized $\Sigma dev^2/dof$ is below 2 should be considered within error margins. Figure S6 thus shows that the best fit value for K_{agg} is 1.4×10^3 M^{-1} with $(0.5\text{-}2.5)\times10^3$ M^{-1} the range of values that should be considered within the error margins. Similarly, ΔH_{agg} is –15.8 kcal mol^{-1} with the range (–40 – –

10) kcal mol^{-1} considered to be within the error margins. Both K_{agg} and ΔH_{agg} are sufficiently well defined for the parameters to be used in the analysis of the ITC data for nucleic acid binding experiments.

ITC study of MB interacting with EAD2

For parallel G-quadruplex EAD2, calorimetry data were analysed in terms of one binding mode combined with ligand self-aggregation (with aggregation as quantified separately – vide supra). Error margins are visualized in Figure S7.

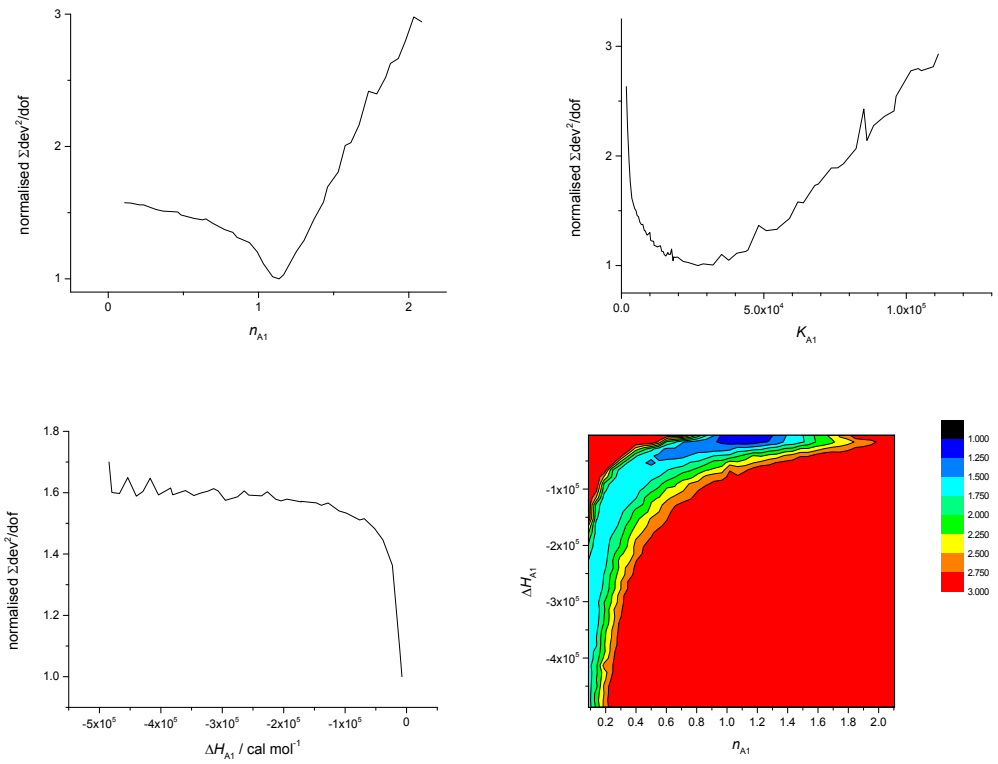

Figure S7

The plots of normalized Σdev²/dof show that the equilibrium constant is reasonably well defined with an optimised value of 2.7 10^4 M^{-1} with reasonable values for K_{A1} in the range of (0.3 – 8.0) 10^4 M^{-1}. ΔH_{A1} and n_{A1} are less well defined as a result of parameter correlation at low values of n_{A1}.

For comparison with the data for MB interacting with HT and TA, we also analyzed the data restricting n_{A1} to a value of 1. This analysis gives normalized Σdev²/dof as a function of K_{A1} as in Figure S8.

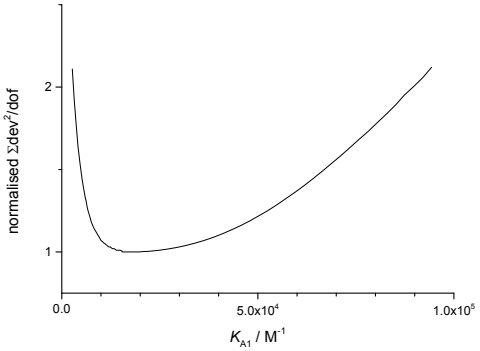

Figure S8

Figure S8 confirms the error margins as resulting from the fit without restricting the value of n_{A1}.

MB interacting with HT

For coexisting or mixed hybrid type HT, calorimetry data were analysed in terms of one binding mode combined with ligand self aggregation (with aggregation as quantified separately – vide supra). Error margins are visualised in Figure S9.

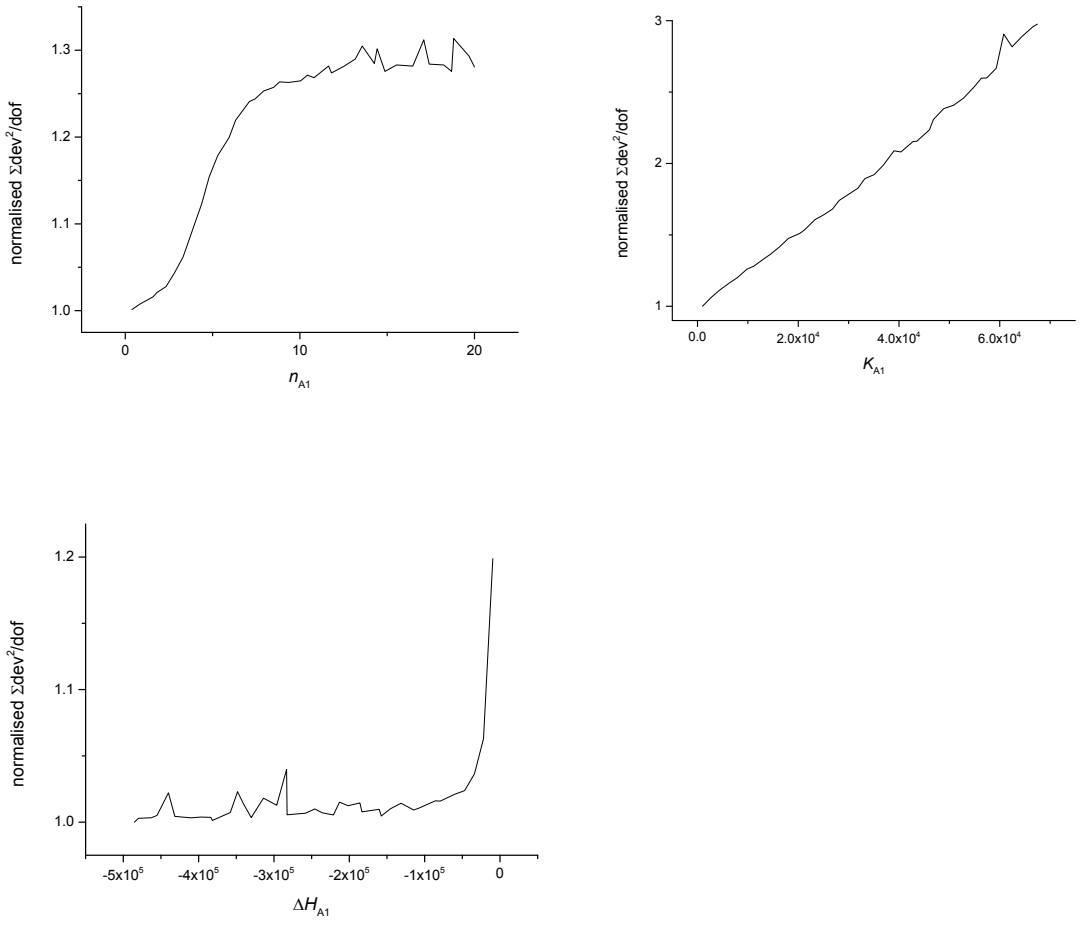

Figure S9

Binding is clearly weak ($K_{A1} < 4\times10^4$ M^{-1}), which for this data set makes it impossible to fully and independently quantify all binding parameters K_{A1}, ΔH_{A1} and n_{A1}.

In order to allow direct comparison with the calorimetry data for MB interacting with EAD2, the data were reanalyzed with the stoichiometry n_{A1} restricted to a value of 1. This analysis generated a range of combinations of K_{A1} and ΔH_{A1} which produce reasonable fits (Figure S10).

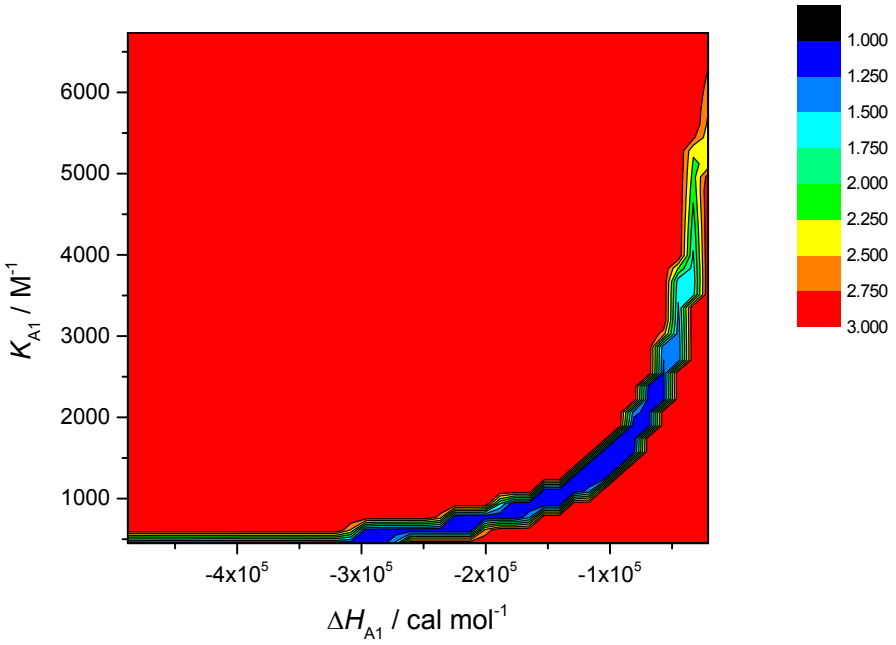

Figure S10

Figure S10 shows that for reasonable values of ΔH_{A1}, *i.e.* $\Delta H_{A1} < 10^5$ M^{-1}, K_{A1} assumes values between 2000 and 6000 M^{-1}.

MB interacting with TA

Based on the shape of the enthalpogram for the titration of TA with MB, calorimetry data were analyzed in terms of two binding modes combined with ligand self-aggregation (with aggregation as quantified separately – vide supra). Parameter correlations are visualized in Figure S11.

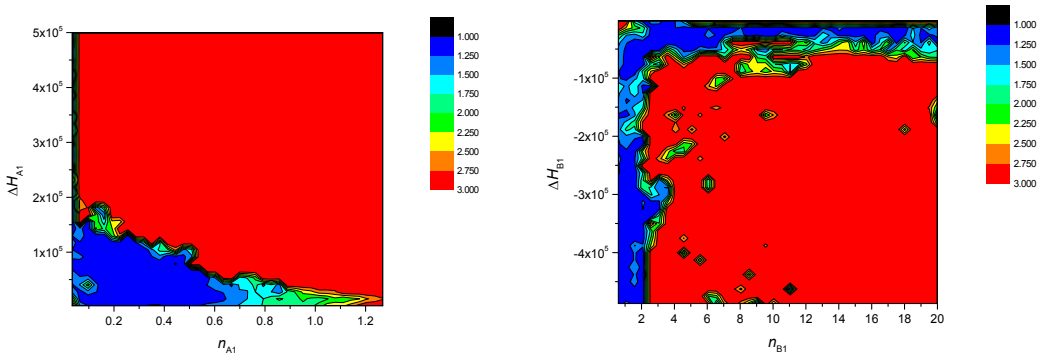

Figure S11

As before, binding is too weak for the individual binding parameters to be fully and independently defined. For comparison, we have therefore again analysed the ITC data restricting the stoichiometry for the first binding event, n_{A1}, to a value of 1. This analysis provides the normalized $\Sigma dev^2/dof$ as a function of K_{A1} as in Figure S12

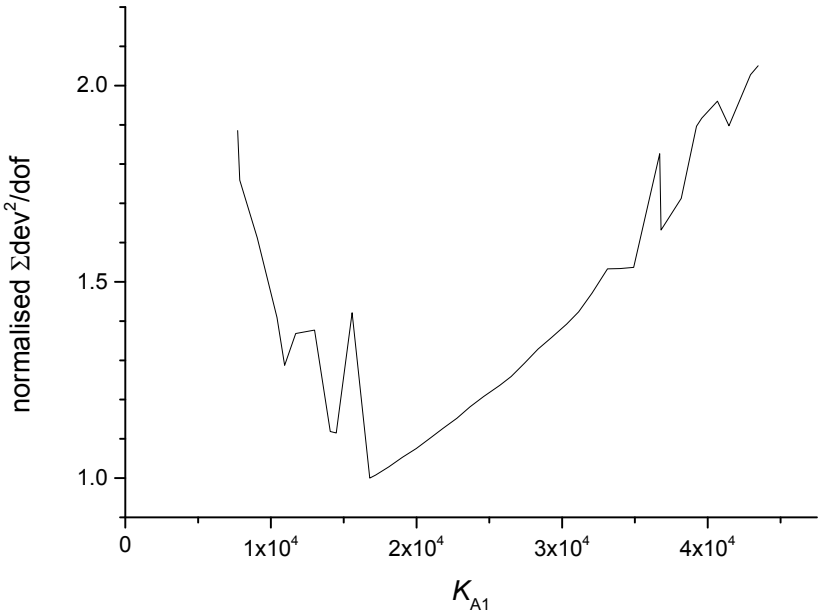

Figure S12

Figure S12 shows that K_{A1} is 1.7 10^4 M^{-1} with the range (0.7-4.2) 10^4 M^{-1} within error margins.

Refences:

1. Macaya, R. F.; Schultze, P.; Smith, F. W.; Roe, J. A.; Feigon, J., Thrombin-binding DNA aptamer forms a unimolecular quadruplex structure in solution. *Proc Natl Acad Sci U S A* **1993,** *90* (8), 3745-3749.
2. Rehder, M. A.; McGown, L. B., Open-tubular capillary electrochromatography of bovine β-lactoglobulin variants A and B using an aptamer stationary phase. *Electrophoresis* **2001,** *22* (17), 3759–3764.
3. Zhou, J.; Yuan, G.; Liu, J.; Zhan, C. G., Formation and stability of G-quadruplexes self-assembled from guanine-rich strands. *Chemistry* **2007,** *13* (3), 945-9.
4. Dai, J.; Chen, D.; Jones, R. A.; Hurley, L. H.; Yang, D., NMR solution structure of the major G-quadruplex structure formed in the human BCL2 promoter region. *Nucleic Acids Res* **2006,** *34* (18), 5133-44.
5. Travascio, P.; Li, Y.; Sen, D., DNA-enhanced peroxidase activity of a DNA aptamer-hemin complex. *Chemistry & Biology* **1998,** *5* (9), 505-517.
6. Cheng, X.; Liu, X.; Bing, T.; Cao, Z.; Shangguan, D., General peroxidase activity of G-quadruplex-hemin complexes and its application in ligand screening. *Biochemistry* **2009,** *48* (33), 7817-23.
7. Sun, D.; Guo, K.; Rusche, J. J.; Hurley, L. H., Facilitation of a structural transition in the polypurine/polypyrimidine tract within the proximal promoter region of the human VEGF gene by the presence of potassium and G-quadruplex-interactive agents. *Nucleic Acids Res* **2005,** *33* (18), 6070-80.
8. Guo, K.; Pourpak, A.; Beetz-Rogers, K.; Gokhale, V.; Sun, D.; Hurley, L. H., Formation of Pseudosymmetrical G-Quadruplex and i-Motif Structures in the Proximal Promoter Region of the RET Oncogene. *J Am Chem Soc* **2007,** *129* (33), 10220-10228.
9. Phan, A. T.; Modi, Y. S.; Patel, D. J., Propeller-Type Parallel-Stranded G-Quadruplexes in the Human c-myc Promoter. *J Am Chem Soc* **2004,** *126* (28), 8710-8716.
10. Fernando, H.; Reszka, A. P.; Huppert, J.; Ladame, S.; Rankin, S.; Venkitaraman, A. R.; Neidle, S.; Balasubramanian, S., A Conserved Quadruplex Motif Located in a Transcription Activation Site of the Human c-kit Oncogene. *Biochemistry* **2006,** *45* (25), 7854-7860.